Bioorganic & Medicinal Chemistry Letters 27 (2017) 4730–4734

Contents lists available at ScienceDirect

Bioorganic & Medicinal Chemistry Letters

journal homepage: www.elsevier.com/locate/bmcl

Discovery of *N*-substituted 7-azaindoles as PIM1 kinase inhibitors – Part I

Claude Barberis [a,*], Neil Moorcroft [a,e], Chris Arendt [b,f], Mikhail Levit [b], Sandra Moreno-Mazza [b,h], Joseph Batchelor [c], Ingrid Mechin [c,g], Tahir Majid [a,d]

[a] IDD Medicinal Chemistry, Sanofi Genzyme, 153 Second Avenue, Waltham MA 02451, USA
[b] Oncology Biochemistry/Biology, Sanofi Genzyme, 270 Albany Street, Cambridge, MA 02139, USA
[c] IDD In Vitro Biology, Sanofi, 153 Second Avenue, Waltham MA 02451, USA
[d] Program Management, Sanofi Genzyme, 49 New York Avenue, Framingham MA 01701, USA

ARTICLE INFO

Article history:
Received 31 May 2017
Revised 25 July 2017
Accepted 31 August 2017
Available online 18 September 2017

Keywords:
PIM1
X-ray crystallography
Inhibitors
Cancer

ABSTRACT

Novel *N*-substituted azaindoles have been discovered as PIM1 inhibitors. X-ray structures have played a significant role in orienting the chemistry effort in the initial phase of hit confirmation. Disclosure of an unconventional binding mode for 1 and 2, as demonstrated by X-ray crystallography, is presented and was an important factor in selecting and advancing a lead series.

The three members of the PIM family of serine/threonine kinases (PIM1, PIM2 and PIM3) were originally identified as Proviral Integration sites in Moloney leukemia virus linked to the survival and proliferation of cancers of hematopoietic origin.[1] They are characterized by a constitutive serine/threonine activity that does not depend upon post-translational modifications for activation.[2] PIM is capable of supporting in vivo tumor proliferation and survival through modification of common, as well as isoform-specific substrates.[3] In normal cells, cytokine signaling through the JAK/STAT pathway strictly regulates the transcriptional activation of the PIM genes and their expression as constitutively active protein kinases. In numerous liquid and solid tumors[4], PIM kinases are over-expressed and this has been associated with drug resistance mechanisms.[4h]

The observation that PIM kinases are selectively over-expressed in certain cancers, while apparently playing non-essential roles in normal cells (as inferred from studies on mice deficient in all three PIM kinases), prompted numerous research groups[5] to initiate medicinal chemistry efforts to identify small molecule inhibitors of PIM kinases. With limited understanding of the exact role of these kinases in human disease, we initiated a high-throughput screening campaign against PIM1 using our proprietary compound collection.

The screening campaign was fruitful, with over thirty confirmed distinct chemical scaffolds inhibiting significantly PIM1 kinase activity at 10 μM. Among these identified scaffolds, a few showed a non-classical ATP-competitive binding mode as confirmed by X-ray crystallography.

Our initial objective in the early phase of the project was to identify compounds for in vitro credentialing studies. To this end, we selected hits on the basis of their chemical originality, potential for derivatization, binding affinity and selectivity profiles. We also wanted to establish a structure-based drug design optimization strategy.

PIM1, 2 and 3 are highly conserved kinases with unique structural properties.[6] Interested by the Pro-123 insertion in the hinge region of the ATP-binding cleft of the preceding kinase, we investigated the molecular interactions of the selected hits with PIM1 by X-ray crystallography. Among co-crystallized structures collected, we were particularly interested by the unexpected interaction observed with compound **A** (light orange, Fig. 1) which is an azaindole derivative. It's binding mode is different from the one

* Corresponding author.
E-mail address: claude.barberis2@sanofi.com (C. Barberis).
[e] Present address: Maxsar Biopharma, 18 Roberts Road, Warren, NJ 07059, USA.
[f] Present address: Takeda, 40 Landsdowne street, Cambridge, MA 02139, USA.
[g] Present address: Icagen, Tucson Research Center, 2090 E. Innovation Park Drive, Oro Valley, AZ 85755, USA.
[h] Present address: PTC Therapeutics, 100 Corporate Court, South Plainfield, NJ 07080, USA.

http://dx.doi.org/10.1016/j.bmcl.2017.08.069
0960-894X/

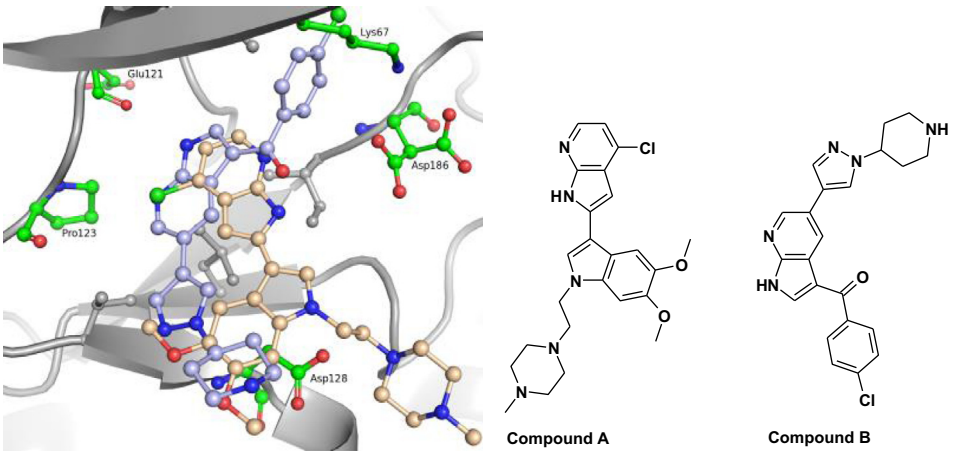

Fig. 1. X-ray crystal structures of 7-azaindoles **A** and **B** respectively bound to PIM1 (orange/5TEL) and PAK1 (Blue/5KBR).

reported for 7-azaindole **B** co-crystallized in the PAK1 kinase active site (Blue, Fig. 1).

In the ATP-binding pocket of PAK1 (Fig. 1, Blue), compound **B** binds as a typical type I ATP-competitive binder with the donor-acceptor motif interacting directly with the hinge. As shown in Fig. 1 (orange), the donor-acceptor motif of compound **A** is facing away from the hinge site and it is the C4-chlorine atom of the aromatic ring that points to this part of the binding pocket. With the exception of a weak and non well-defined interaction with Asp-131via the piperazine motif, compound **A** does not show any obvious direct contact with PIM1. This binding mode was further confirmed with other 7-azaindole hits such as compound **1** in Fig. 2 exhibiting this "reverse" binding mode in PIM1 as shown in Fig. 3.

Knowing that the azaindole N1-H was not involved in a classical bidentate H-bond interaction with PIM1, we decided to modify this part of the molecule with the objective to improve potency and reduce off-target kinase activity. To this end, compounds **1** and **3** (Fig. 2) which had modest potencies on PIM1 (1.03/2.5 μM) and ligand efficiencies (LE = −0.37), and cross-reacting against cell cycle kinases such as CDK9 and CDC7 was converted to compounds **2** and **4** (Fig. 2) using the synthetic chemistry approach described in Schemes 1 and 2.

The new derivatives **2** and **4** maintained the original potencies towards PIM1 (IC50 ~1 μM) and also retained the original binding mode (Fig. 3), but showed a much improved selectivity against CDK9 and CDC7. The binding mode of compounds **1**–**4** confirmed that cross-reactivity with the kinome would not be an issue. This enabled us to synthesize highly selective tool compounds to interrogate PIM biology.[7]

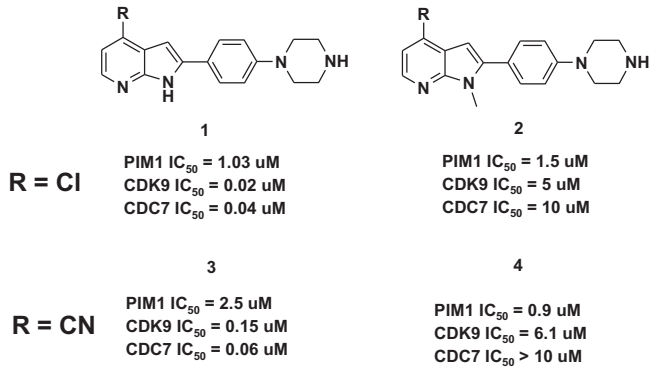

Fig. 2. Comparison of the selectivity of 4-cyano/chloro-7-azaindoles 1–4 towards CDK9 and CDC7.

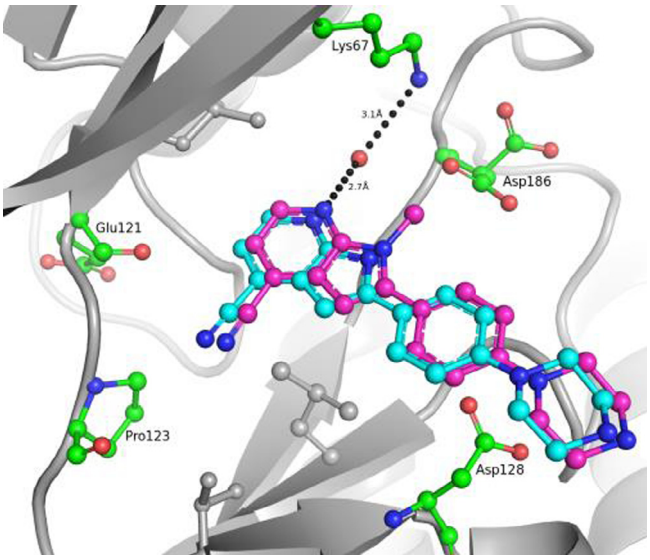

Fig. 3. Superimposition of two X-ray crystal structures of compounds **3** (Blue/5TOE) and **4** (purple/5TUR) bound to PIM1.

Encouraged by these initial results, and given that the 7-azaindole scaffold offered interesting possibilities for a multi-dimensional optimization approach, we initiated medicinal chemistry around the 4-chloro-7-azaindole chemotype. Scheme 1 outlines our synthetic strategy to introduce chemical diversity. We desired a flexible synthetic approach for developing a spectrum of analogs for this series. The synthesis of intermediate **8** (Scheme 1), which proved to be accessible in large quantities, was key to our strategy.

Commercially available 7-azaindole was treated with mCPBA to provide compound **5** as a salt. The free base *N*-oxide was released at pH 9 by treatment with an aqueous solution of K_2CO_3. The *N*-oxide **5** was treated with $POCl_3$ to provide Cl-azaindole **6** regioselectively in reasonable yields. The N1 nitrogen was protected with a MOM group to produce **7**. The directing group helped provide **8** in reproducibly high yield. Intermediate **8** was used as a central template to diversify chemistry at C2, C3 and N1 positions, as needed.

Deprotection of **8** (Scheme 2) using bromo-catecholborane proved to be a slow 2-stage process to ultimately give **9**. Alkylation at N1 gave *N*-methyl derivative **10**, which underwent a smooth cross-coupling at *C*2 to provide intermediate **11**. Iodination at C3 to give **12** followed by Suzuki coupling yielded **13**. Final targets were accessed from intermediates **7**, **8**, and **12** as needed.[8]

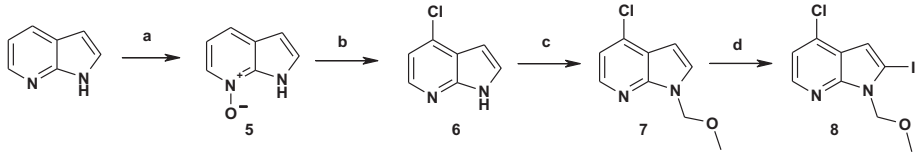

Scheme 1. Reagents and conditions: (a) mCPBA, DME/heptane, 89%; (b) $POCl_3$, 100 °C, 80%; (c) Bu_4NHSO_4, NaOH, MOM-Cl, MeCN, 75%; (d) LDA, THF, I_2, 91%.

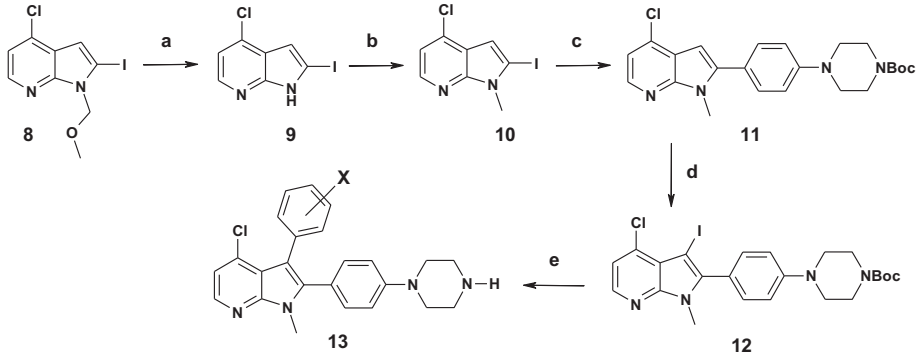

Scheme 2. Reagents and conditions: (a) Br-catecholborane, DCM, followed by NaOH; (b) NaH, DMF, MeI, 80% two steps; (c) $Pd(PPh_3)_4$, boronate, Cs_2CO_3, DME/H_2O, 75%; (d) THF/MeOH, NIS, 95%; (e) i) step c); ii) EtOH, HCl.

Biochemical IC_{50} measurements[i] for PIM1, 2 and 3 were obtained using a TR-FRET assay with full-length human BAD substrate. While most of the compounds showed double-digit nanomolar activity against PIM1, potency against PIM2 was in comparison significantly lower. This can be explained by the difference in Km for ATP between these enzymes. We found using a radioactive filter-binding assay ATP Km = 67, 5.4, 97 μM for PIM1, 2 and 3 respectively.[j] Surprisingly, PIM3 inhibition was comparable to PIM2 for this set of compounds which could not be explained by structural biology.

In fact, while this initial exploration led to PIM1 biochemical potencies below 100 nM, it was only achieved using large basic moieties at C3 and/or C2 reaching water exposed-region, and was usually accompanied by a two log difference for PIM2 and PIM3, as shown in Scheme 3 for representative compounds.

Having identified a series of PIM1-specific inhibitors, we next performed the evaluation for a few of them in a panel of cancer cell lines to try to understand the biological impact of PIM1 inhibition.

The proliferative inhibition induced by compounds **14** and **15** across a number of liquid and solid tumor cancer cell lines is shown in Table 1. Results were modest, with the best potency observed in the colon cancer cell lines HCT-116 and HT-29.

Compound **15** was selected to be screened against an internal panel of 49 representative kinases at 10 μM which demonstrated a selective series (data not shown) with weak cellular potency. Given the additional expression of PIM2 and/or PIM3 in numerous cancers, we surmised that selective inhibition of PIM1 may be insufficient to efficiently inhibit cellular growth, and that a pan-PIM inhibitor may be required to overcome PIM pathway-mediated pro-survival processes associated with tumorogenesis.

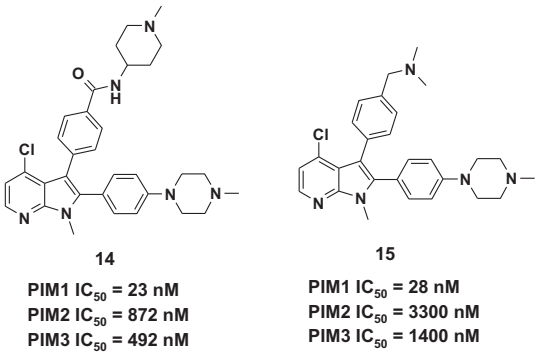

Scheme 3. Representative hits obtained after initial analoging.

At this point, we turned our attention to the last unexplored position of the 7-azaindole, namely position 6. This position was initially set aside due to the lack of optimizable space, based on the X-ray data. However, this position was proximal to Glu-121 carbonyl so compounds **19** and **20** were designed to target it as shown in Scheme 4.

While compound **20** was found inactive with a PIM1 IC_{50} above 10 μM, we observed that **19** had a PIM1 IC_{50} of 250 nM, about four-fold more potent than compound **2**. Of note, this was achieved without a substituent at C3, previously found to improve potency at least ten fold.

Interestingly, even though PIM2 potency for **19** was still in the high micromolar range, PIM3 biochemical IC_{50} was now 400 nM. Equipotency between PIM1 and PIM3, while initially expected and desired, was not attained until now.

To further investigate the increase in PIM1 inhibitory potency of **19**, we generated compounds **21** and **22** (Scheme 5). To our surprise, **21** lost PIM1 potency (IC_{50} >30 μM), while **22** exhibited a further 10-fold increase in PIM1 potency. We once again turned our attention to X-ray crystallography to understand these results.

As shown in Fig. 4, newly synthesized **24** (Yellow) had rotated 60° clockwise in the PIM1 binding pocket, compared to analog **23** (Pink). This rotation was presumably triggered by an hydrogen bond of the C6 carboxamide with the catalytic Lys-67. Such an

[i] IC_{50} against PIM1, PIM2, and PIM3 kinases was routinely tested using an in vitro TR-FRET assay based on detection of phosphorylation of specific Ser112 residue in Bad protein. Final reaction mixtures (40 μL) contained 2 nM PIM proteins, 50 nM Bad, 40 μM ATP, and dilutions of the tested compounds in reaction buffer.

[j] Apparent K_m (ATP) for PIM1, PIM2, and PIM3 were measured using radiolabeling filter-binding assay. Reaction mixtures containing 2 nM Pim proteins, 100 μM substrate peptide Pim2tide representing amino-acids 107–117 of mouse BAD, and varying concentrations of ^{33}P-ATP in reaction were incubated at ambient temperature. The level of ^{33}P-Pim2tide was quantified using a TopCount plate reader (PerkinElmer).

Table 1
Cancer cell line proliferative inhibition by **14** and **15**.

	EOL-1	MOLM-13	MV4-11	K-562	HCT-116	HT-29	H460	PC3
EC_{50} **14** (μM)	0.8	1.1	1.3	1.3	0.2	0.3	1.1	1.0
EC_{50} **15** (μM)	0.5	0.6	0.6	1.1	0.1	0.1	1.0	0.8

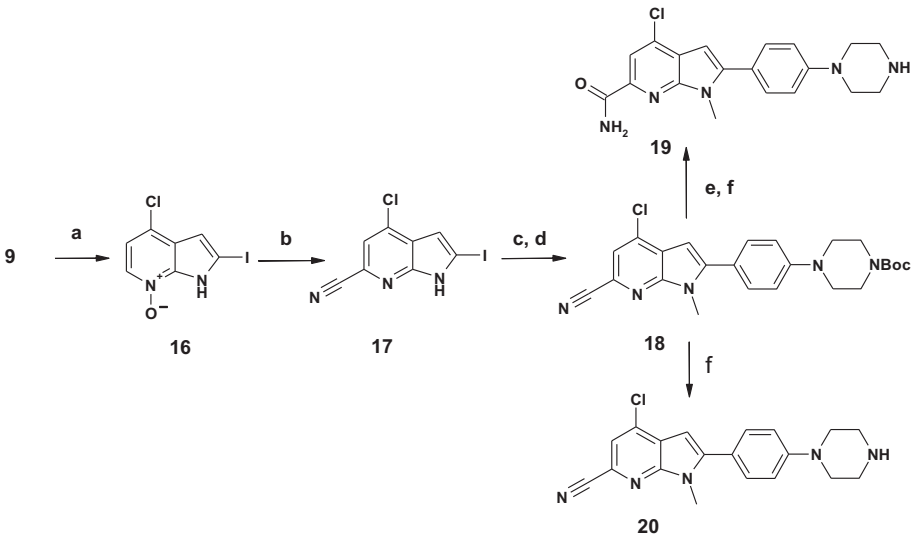

Scheme 4. Reagents and conditions: (a) mCPBA, AcOEt; (b) TMSCN, Et_3N, ACN; (c) NaH, DMF, MeI; (d) $Pd(PPh_3)_4$, Boronate, Cs_2CO_3, DME/H_2O; (e) TMSOK, THF; (f) TFA, DCM.

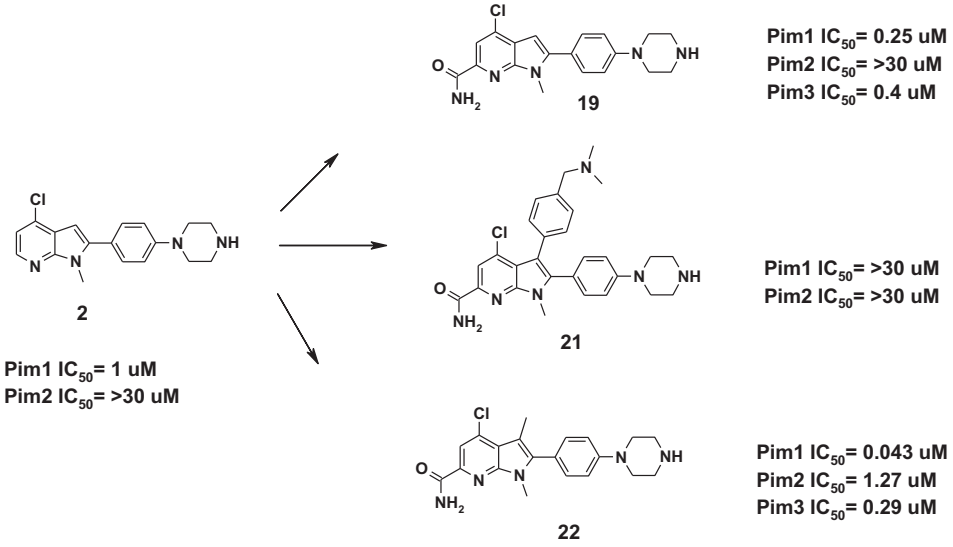

Scheme 5. Synthesis of C6-substituted 7-azaindoles.

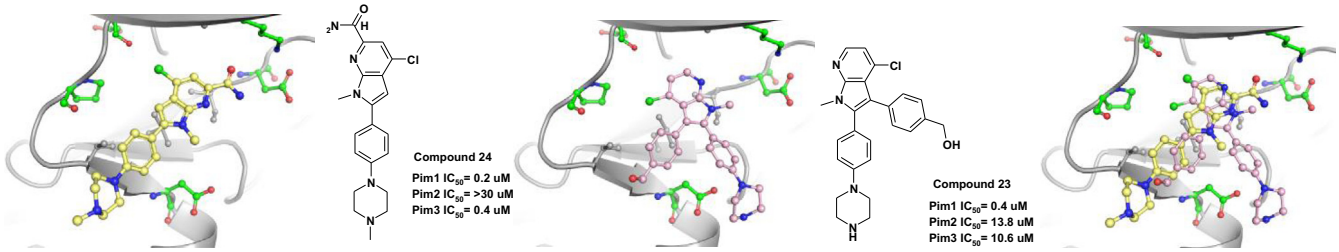

Fig. 4. X-ray crystallography of **24** (Yellow/5KCX) and analog **23** (Pink/5TEX), plus overlaid in PIM1.

interaction was not possible with any of the previous analogs. This repositioning of the scaffold explained the biochemical results observed and opened new opportunities to design compounds that might inhibit all three PIM enzymes.

We now had inhibitors with two distinct interactions with the protein, one of which pointed the C4-chlorine towards Glu-121, generating an interesting halogen bonding interaction.[9] The second of these interactions was mediated by the C6 carboxamide binding to the conserved Lys-67 of PIM1. The C3 position of the azaindole core was now facing the hinge with limited space to accommodate substituents, which explained the lack of PIM1 potency for **21** and **23** used for crystallography. The newly oriented molecule presented a direct access to the aspartate cluster (Asp-128, Asp-131 and Glu-171) from the N1 position, offering an opportunity to optimize inhibitory potency on PIM2.

In summary, we report the discovery of original PIM1 kinase inhibitors. Although the initial SAR with this chemical series was disappointing, we uncovered a change from the original binding mode, which permitted us to re-orient our efforts towards the discovery of a lead series. The initial objectives were thus attained, namely identifying a hit series with specific interactions with the Lys-67 and Glu-121, but in a non-typical hinge-binding modality. We also discovered that we could access the ribose-binding pocket, which might improve potency on PIM2. Exploitation of this new binding mode towards finding a pan-PIM lead series is described in the accompanying Parts.

Acknowledgments

The authors thank Isabelle Morize and Kimberly Haas for their contribution to molecular modeling and Peter Hamley's team in Frankfurt for compound library synthesis support. We also thank Jean-Paul Nicolas for the evaluation of compounds on solid tumors panel.

References

1. (a) Nawijin MC, Alendar A, Berns A. *Nat Rev Cancer*. 2011;11:23;
(b) Brault L, Gasser C, Bracher F, Huber K, Knapp S, Schwaller J. *Haematologica*. 2010;95:1004;
(c) Bachmann M, Kosan C, Xing PX, Montenarh M, Hoffmann I, Moroy T. *Int J Biochem Cell Biol*. 2006;38:430.
2. (a) Qian KC, Wang L, Hickey ER, et al. *J Biol Chem*. 2005;280:6130;
(b) Bullock AN, Debreczeni JE, Amos AL, Knapp S, Turk BE. *J Biol Chem*. 2005;280:41675.
3. (a) Morishita D, Katayama R, Sekimizu K, Tsuruo T, Fujita N. *Cancer Res*. 2008;68:5076;
(b) Gong J, Wang J, Ren K, Liu C, Li B, Shi Y. *J Surg Res*. 2009;153:17.
4. (a) Amson R, Sigaux F, Przedborski S, Flandrin G, Givol D, Telerman A. *Proc Natl Acad Sci USA*. 1989;86:8857;
(b) Warnecke-Eberz U, Bollschweiller E, Drebber U, et al. *Anticancer Res*. 2009;29:4451;
(c) Mumenthaler SM, Ng PY, Hodge A, et al. *Mol Cancer Ther*. 2009;8:2882;
(d) Cohen AM, Grinblat B, Bessler H, et al. *Leuk. & Lymphoma*. 2004;45:951;
(e) Breuer LM, Cuypers HT, Berns A. *EMBO J*. 1989;8:743;
(f) Zheng HC, Tsuneyama K, Takahashi H, et al. *J Can Res Clin Oncol*. 2008;134:481;
(g) Li Y, Popivanova BK, Nagai Y, Ishikura H, Fujii C, Mukaida N. *Cancer Res*. 2006;66:6741;
(h) Isaac M, Siu A, Jongstra J. *Drug Res*.. 2011;14:203.
5. (a) Morwick T. Expert. *Opin. Ther. Pat*.. 2010;20:193. and references therein;
(b) Drygin D, Haddach M, Pierre F, Rychman DM. *J Med Chem*. 2012;55:8199;
(c) Nishiguchi GA, Atallah G, Bellamacina C, et al. *Bioorg Med Chem Lett*. 2011;21:6366;
(d) Pierre F, Stefan E, Nedellec AS, et al. *Bioorg Med Chem Lett*. 2011;21:6687;
(e) Pastor J, Oyarzabal J, Saluste G, et al. *Bioorg Med Chem Lett*. 2012;22:1591;
(f) Tsuhako AL, Brown DS, Koltun ES, et al. *Bioorg Med Chem Lett*. 2012;22:3732;
(g) Dakin LA, Block MH, Chen H, et al. *Bioorg Med Chem Lett*. 2012;22:4599;
(h) Nakano H, Saito N, Parker L, et al. *J Med Chem*. 2012;55:5151;
(i) Lukasik PM, Elabar S, Lam F, et al. *Eur J Med Chem*. 2012;57:311;
(j) Casuscelli F, Ardini E, Avanzi N, Casale E, et al. *Bioorg Med Chem*. 2013;21:7364;
(k) Suchaud V, Gavara L, Saugues E, et al. *Bioorg Med Chem*. 2013;21:4102;
(l) Wang X, Magnuson S, Pastor R, et al. *Bioorg Med Chem Lett*. 2013;23:3149;
(m) Ishchenko A, Zhang L, LeBrazidec JY, et al. *Bioorg Med Chem Lett*. 2015;25:474;
(n) Wang H-L, Cee VJ, Chavez Jr F, et al. S. *Bioorg Med Chem Lett*. 2015;25:834;
(o) Wurz RP, Sastri C, D'Amico DC, et al. *Bioorg Med Chem Lett*. 2016;26:5580;
(p) Nishiguchi GA, Burger MT, Han W, et al. *Bioorg Med Chem Lett*. 2016;26:2328;
(q) Pettus LH, Andrews KL, Booker SK. *J Med Chem*. 2016;59:6407;
(r) Burger MT, Nishiguchi G, Han W, et al. *J Med Chem*. 2015;58:8373;
(s) Burger MT, Han W, Lan J, et al. *Bioorg Med Chem Lett*. 2013;4:1193.
6. (a) Kumar A, Mandiyan V, Suzuki Y, et al. *J Mol Biol*. 2005;348:183;
(b) Jacob MD, Black J, Futer O, et al. *J Biol Chem*. 2005;280:13728.
7. Guo Z, Wang A, Zhang W, et al. *Blood*. 2014;124:1777.
8. Arendt C, Barberis C, Levit M, Majid TN, WO2011075613.
9. Wilcken R, Zimmermann MO, Lange A, Joerger AC, Boeckler FM. *J Med Chem*. 2013;56:1363.